

Adaptive Sliding Window Minimum Mean Square Error Inter-Carrier Interference Cancellation

Rana Ahmed
Institute of Telecommunications
University of Stuttgart
rana.salem@inue.uni-stuttgart.de

Nabil Sven Loghin
Sony Deutschland GmbH
European Technology Center (EuTEC)
nabil.loghin@eu.sony.com

Joachim Speidel
Institute of Telecommunications
University of Stuttgart
joachim.speidel@inue.uni-stuttgart.de

Abstract—Channel variation causes a loss of orthogonality among the subcarriers of an Orthogonal Frequency Division Multiplexing (OFDM) symbol and leads to inter-carrier interference (ICI) and degradation in performance. In this work, we propose a minimum mean square error ICI canceller with an adaptive sliding window (MMSE-ASW). In a frequency selective channel, the proposed MMSE-ASW adopts a different window size depending on the degree of ICI to which each subcarrier is subjected relative to the power of the signal part. A metric is computed for each subcarrier to determine the degree of interference which depends on the estimated ICI coefficients. A closed form is derived to get the optimum value of the window size used in the MMSE-ASW approach. We analyze the performance and the complexity trade-off of the algorithm. We demonstrate the effectiveness of the proposed method for a frequency selective fast fading channel, in a first generation digital video broadcasting system (DVB-T). As a result, we found that at a Doppler frequency of 100Hz, the proposed algorithm requires only about 32% of the complexity needed in the conventional MMSE approach to deliver the same bit error rate (BER) performance.

I. INTRODUCTION

OFDM has emerged as an attractive modulation scheme in many digital broad-band standards. It has the advantage of being robust in frequency selective channels along with a simple transceiver structure. An OFDM data stream is de-multiplexed into N parallel low rate substreams, which are modulated over N subcarriers. The bandwidth of each modulated subcarrier is small enough to assume a frequency flat fading channel. A guard interval (cyclic prefix) is inserted between successive OFDM symbols. If the channel impulse response is shorter than the length of the guard interval, inter-symbol interference (ISI) is eliminated. In a time invariant channel, a one-tap zero forcing (ZF) equalizer can then recover the transmitted symbol on each subcarrier. However, the orthogonality among the OFDM subcarriers is destroyed when the OFDM symbol is transmitted over time-varying channels, resulting in ICI. The longer the duration of the OFDM symbol, the more sensitive it is to a time-varying channel. In DVB-T [1], an OFDM size up to 8k subcarriers is used, and such a symbol lasts for about 1ms when used in an 8MHz channel.

In a wireless environment, the channel can be time-varying because of statistical multi-path propagation and the mobility of the user. The maximum Doppler frequency $f_{D,max}$ and normalized maximum Doppler frequency $f_{D,norm}$ are given

by

$$f_{D,max} = \frac{f_c v}{c}, \quad (1)$$

$$f_{D,norm} = \frac{f_{D,max}}{\Delta f} \quad (2)$$

where f_c is the RF carrier frequency, v is the velocity of the user, c is the speed of light and Δf is the subcarrier spacing. In the rest of this paper, we drop the term 'maximum' when referring to the maximum Doppler frequency or the normalized maximum Doppler frequency. For more information about modeling a time-varying multi-path channel, the interested reader can refer to [2]. ICI can also arise because of unknown carrier frequency offset between the local oscillators at the transmitter and the receiver. In [3], in order to mitigate this problem, the subcarrier frequency offset is estimated and then compensated for. In our work, we focus on the problem of ICI as a result of a time-varying channel.

A well known linear receiver used to mitigate ICI is a minimum mean square error (MMSE) equalizer. In [4] and [5], a low complexity sliding window MMSE receiver is proposed with a window size much smaller than the Fast Fourier Transform (FFT) size. This approach has the advantage of lowering the required complexity for equalizing an OFDM symbol from $O(N^3)$ to $O(NK^3)$, where N and K are the FFT size and the selected window size, respectively. The larger the size of the window, the better the performance is, which can be achieved with the equalizer, at the expense of a higher complexity. In [5], this approach was combined with successive interference cancellation (SIC). However, in [4] and [5], a constant window size was used for all OFDM subcarriers within an OFDM symbol.

In our work, we propose to choose the size of this window dynamically according to the subcarrier's signal to interference ratio. We demonstrate that the signal to interference ratio is frequency selective in a multi-path channel. Thus, it is advantageous to use different values of the window size for the different subcarriers. While the conventional approach in [4] uses one value for the window size for all subcarriers, we propose to use different values for the window size for the different subcarriers to achieve a better trade-off between BER performance and complexity. In order to optimize the BER performance vs complexity tradeoff, we derive a closed form formula to compute the adaptive window size per subcarrier

such that a prescribed minimum threshold of the signal to interference ratio is met.

This paper is organized as follows: in section II, we introduce the system model and the ICI problem due to a time varying channel. In section III, we describe the conventional MMSE ICI canceller. In section IV, a simplified formula for the signal to interference ratio is derived. In section V, we describe the proposed adaptive sliding window MMSE receiver. In section VI, we analyze the complexity of the conventional and the proposed MMSE equalizer. In section VII, we present simulation results which show the effectiveness of the proposed MMSE-ASW approach for a doubly selective channel.

II. SYSTEM MODEL

The signal vector after the FFT at the receiver side, $\mathbf{R}_{N \times 1}$, can be written in matrix form as

$$\mathbf{R} = \mathbf{H}\mathbf{S} + \mathbf{X}, \quad (3)$$

where \mathbf{H} is the 2D Discrete Fourier Transform (DFT) of the $N \times N$ time domain channel matrix \mathbf{H}_t [6], \mathbf{S} is the vector of transmitted symbols and \mathbf{X} is the effective frequency domain additive white Gaussian noise (AWGN) vector. The channel matrix \mathbf{H} can thus be computed as

$$\mathbf{H} = \mathbf{F}\mathbf{H}_t\mathbf{F}^H, \quad (4)$$

where \mathbf{F} is the DFT matrix and $()^H$ denotes the Hermitian operation. \mathbf{H} is composed of the elements $H(k, l)$, $k, l = 1, \dots, N$. In case of a time-invariant channel, \mathbf{H}_t is a circulant matrix, and hence its 2D DFT, \mathbf{H} , is a diagonal matrix. The k^{th} element $R(k)$ of \mathbf{R} , can then be written as

$$R(k) = H(k, k)S(k) + X(k), \quad (5)$$

where $S(k)$ and $X(k)$ are the sent symbol and the effective frequency domain noise for subcarrier index k , respectively. $H(k, k)$ is the k^{th} element on the main diagonal of \mathbf{H} . For a time-invariant channel, a one-tap ZF equalizer is sufficient to estimate $S(k)$. In case of a time-varying channel, the off-diagonal frequency coefficients in \mathbf{H} are no longer zero. The larger the Doppler frequency, the larger the power leaking to the off-diagonal coefficients is. In Fig. 1, we can see the normalized magnitudes of the 16 DFT channel matrix coefficients for a frequency flat Rayleigh fading channel at two different normalized Doppler frequency values. The coefficients' magnitudes are normalized with respect to the magnitude of the largest main diagonal element $|H|_{max}$, $H_n(k, l) = \frac{H(k, l)}{|H|_{max}}$. As shown in Fig. 1, if the Doppler frequency increases, the magnitudes of the interference off-diagonal coefficients increase. Consequently, ICI induces a higher error floor on the BER performance [7].

III. MINIMUM MEAN SQUARE ERROR RECEIVER

In this section, we describe an OFDM receiver which can reduce the effect of ICI. Recalling the linear equation in (3), an MMSE receiver minimizes the following cost function

$$\|\mathbf{S} - \hat{\mathbf{S}}\|^2, \quad (6)$$

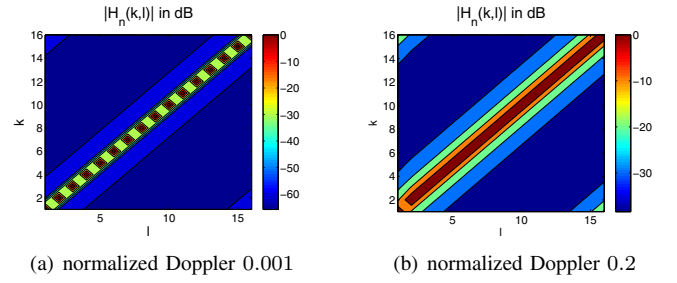


Fig. 1. Normalized matrix coefficients $\frac{|H(k, l)|}{|H|_{max}}$ of frequency flat fading channel matrix \mathbf{H} at different Doppler frequencies

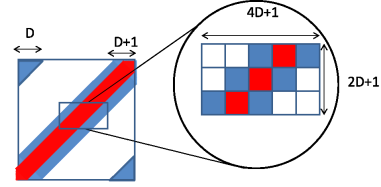


Fig. 2. Channel matrix structure and sliding window

where the detected symbol vector $\hat{\mathbf{S}}$ is computed as: $\hat{\mathbf{S}} = \mathbf{W}\mathbf{R}$. \mathbf{W} is the $N \times N$ MMSE matrix computed as in [8]

$$\mathbf{W} = (\mathbf{H}^H\mathbf{H} + \sigma_x^2\mathbf{I})^{-1}\mathbf{H}^H, \quad (7)$$

where σ_x^2 is the AWGN variance and \mathbf{I} is the identity matrix. At high DFT size, N , the prohibitive complexity of (7) motivates the use of a sliding window as proposed in [4]. As shown in Fig. 2, a sliding window, $\mathbf{H}'(k)$, of size $(2D+1) \times (4D+1)$ is centered around the k^{th} main diagonal element $H(k, k)$, such that a limited number of interference off-diagonal coefficients are considered. D is the number of off-diagonals in each direction around the main diagonal inside the window, where $D \in \{1, 2, \dots, 0.5N\}$. In other words, at every subcarrier index, k , 2D neighboring interferers are considered and the rest are assumed to be zero. The channel submatrix $\mathbf{H}'(k)$ at subcarrier position k is formed out of the elements in the $N \times N$ channel matrix \mathbf{H} as

$$\mathbf{H}'(k) = \begin{bmatrix} H(k-D, k-2D) & \dots & H(k-D, k+2D) \\ \vdots & \vdots & \vdots \\ H(k, k-2D) & \dots & H(k, k+2D) \\ \vdots & \vdots & \vdots \\ H(k+D, k-2D) & \dots & H(k+D, k+2D) \end{bmatrix} \quad (8)$$

The main operations carried out by the MMSE equalizer per subcarrier position k can be written as

- 1) Build the filtering vector $\mathbf{C}(k)$ as

$$\mathbf{C}(k) = (\mathbf{H}'(k)(\mathbf{H}'(k))^H + \sigma^2\mathbf{I})^{-1}\mathbf{A}(k), \quad (9)$$

where $\mathbf{A}(k)$ is the middle column of the matrix $\mathbf{H}'(k)$.

- 2) Multiply the window of the received samples $\mathbf{R}'(k) = [R(k-D) \dots R(k+D)]^T$ by the filter $\mathbf{C}(k)$, tak-

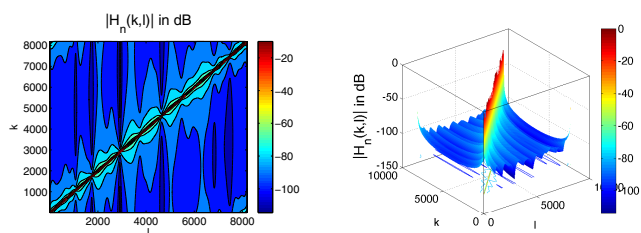
ing into account the required normalization factor

$$\hat{S}(k) = \frac{1}{\mathbf{C}^H(k)\mathbf{A}(k)}\mathbf{C}^H(k)\mathbf{R}'(k), \quad (10)$$

where $()^T$ denotes the transpose operation. The required complexity is then $O(N(2D+1)^3)$ instead of $O(N^3)$ in case the full MMSE matrix is computed. As the Doppler frequency increases, more off-diagonals should be considered in the computation of the MMSE receiver vector $\mathbf{C}(k)$. However, as the number of off-diagonals considered increases, the complexity also increases exponentially.

In Fig. 1, we notice the Toeplitz channel matrix structure, i.e. all elements on the same off-diagonal have the same value. This is true only for a frequency flat channel, where all the coefficients change with the same rate. Fig. 3 depicts the magnitudes of the normalized coefficients $|H_n(k, l)|$ for a frequency selective channel, namely the Typical Urban 6 tap channel (TU6) as defined in [9], using an 8k DFT. As shown, the frequency selectivity is visible in the main diagonal, as well as for the off-diagonal coefficients. In this work, we propose to use a sliding window MMSE ICI canceller which takes the frequency selectivity into account. As pointed out earlier, the complexity of the MMSE approach increases exponentially with the window size, therefore we propose to use large window sizes only when needed. The proposed ICI canceller uses an adaptive window size to mitigate the interference on every subcarrier signal depending on the degree of interference to which it is subjected. In other words, subcarrier signals with low interference conditions use a small value of D and therefore consume fewer number of multiplications in the equalizer block, whereas those which suffer from high interference choose a higher value of D . The criteria by which the window size is chosen will be explained in the next section.

IV. THE SIGNAL TO INTERFERER RATIO



(a) 2D plot of the channel matrix (b) 3D plot of the channel matrix

Fig. 3. 2D and 3D plot of normalized matrix coefficients $\frac{|H(k,l)|}{|H|_{max}}$ of a TU6 channel matrix \mathbf{H} at a normalized Doppler frequency of 0.2

We define the signal to interferer ratio (SIR) as the ratio of the squared magnitude of the main diagonal element of the channel matrix at subcarrier position k , $|H(k, k)|^2$, to the square of the sum of magnitudes of the channel coefficients at $(k, k \pm D)$

$$SIR_D(k) = \frac{|H(k, k)|^2}{|I_D(k)|^2}, \quad (11)$$

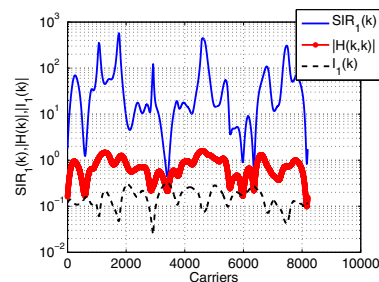


Fig. 4. Frequency selectivity of SIR_1 on a TU6 channel at a normalized Doppler frequency of 0.2

where the interference function $I_D(k)$ is defined as the average interference magnitude obtained from the two interferers that are D subcarriers apart from the current subcarrier position k in both directions.

$$I_D(k) = 0.5 (|H(k, k + D)| + |H(k, k - D)|) \quad (12)$$

Our aim is to obtain a signal to interference ratio function which is monotonically increasing with the number of subcarriers considered D , i.e. the signal to interference ratio function should increase as D increases. This is why we define the interference function using only the contribution of the D^{th} neighboring subcarriers instead of a cumulative sum of all interferers up to the D^{th} neighboring subcarriers.

In a frequency flat fading channel, the SIR is constant along the off-diagonal. In a frequency selective channel, on the other hand, the SIR is also frequency selective. This is demonstrated in Fig. 4 for a TU6 channel, which depicts $SIR_D(k)$ for $D = 1$, the magnitudes of the main diagonal $|H(k, k)|$ and the magnitude of the interference function at $D = 1$, $I_1(k)$.

In practice, pilot symbols are sent and used to calculate an estimate of the channel. The pilot assisted channel estimate (PACE) yields an estimate of the main diagonal of the channel matrix, i.e. $H^{PACE}(k) \approx H(k, k)$. In [10], the main diagonal coefficients, $H(k, k) \forall k \in \{1, \dots, N\}$, are assumed to change linearly from 1 OFDM symbol to the next according to a linear function $\alpha(k)$. The off-diagonal coefficients are computed based on the temporal rate of change of the main diagonal coefficients between two successive OFDM symbols. Let $H^y(k, l)$ denote the channel coefficient at the time instant when the y^{th} OFDM symbol is transmitted. The off-diagonal coefficients are then computed as:

$$H^y(k, k + d) = \begin{cases} \frac{\alpha^{-1}(k+d) + \alpha^1(k+d)}{2(1 - \exp(\frac{j2\pi d}{N}))} & \text{even } d \\ \frac{\alpha^{-1}(k+d) + \alpha^1(k+d)}{2(1 - \exp(\frac{j2\pi d}{N}))} + \frac{2(\alpha^{-1}(k+d) - \alpha^1(k+d))}{N(1 - \exp(\frac{j2\pi d}{N}))^2} & \text{odd } d \end{cases} \quad (13)$$

where the slopes $\alpha^x(k)$ are computed using the previous ($x = -1$) and the following ($x = 1$) OFDM symbols as

$$\alpha^x(k) = \text{sign}(x) \frac{H^{y+x}(k, k) - H^y(k, k)}{N}. \quad (14)$$

For high DFT sizes, N , we can neglect the second term in the computation of the odd off-diagonal coefficients in (13),

leading to an approximation of (11)

$$SIR_D(k) \approx \left(\frac{|H(k, k)| |4(1 - \exp(\frac{-j2\pi D}{N}))|}{|g(k-D) + g(k+D)|} \right)^2, \quad (15)$$

where $g(k) = \alpha^{-1}(k) + \alpha^1(k)$. Using (15), the SIR can be computed for all subcarriers by means of PACE.

V. ADAPTIVE SLIDING WINDOW MMSE ICI CANCELLER

We seek in the following a closed form for $D(k)$ by applying some approximations on (15). For $D \ll N$, we can use the following approximation $|4(1 - e^{\frac{-j2\pi D}{N}})| \approx \frac{8\pi D}{N}$ in (15). $SIR_D(k)$ can then be written as

$$SIR_D(k) \approx \left(\frac{|H(k, k)|}{|g(k-D) + g(k+D)|} \frac{8\pi D}{N} \right)^2, \quad (16)$$

We propose to choose a dedicated D depending on $SIR_D(k)$ such that $SIR_D(k) > SIR_{min}$, where SIR_{min} is a predefined threshold. Using (16) directly to compute the suitable D requires several iterations over D . However, for $D \ll N$, which is true for large DFT sizes, we can assume that $g(k-D) \approx g(k) \approx g(k+D)$. In such case, we can approximate (16) as

$$SIR_D(k) \approx \left(\frac{|H(k, k)|}{|g(k)|} \frac{4\pi D}{N} \right)^2. \quad (17)$$

The optimum D can then be found as

$$D(k) \approx \text{round} \left(\frac{N \sqrt{SIR_{min}} |g(k)|}{4\pi |H(k, k)|} \right). \quad (18)$$

With (18), our proposed MMSE-ASW algorithm chooses the window size parameter $D(k)$ adaptively for each k .

VI. COMPLEXITY ANALYSIS

In this section, we analyze the complexity per subcarrier of the MMSE equalizer using (10). In the following, we determine the complexity only based on the number of multiplications. We assume the division operation such as the one in (18) to be more complex than that of multiplication. We make a reasonable assumption that one division operation is three times more complex than one multiplication operation. $D(k)$ can be determined through 1 division operation, $\frac{|g(k)|}{|H(k, k)|}$, where $D(k)$ can be determined using a look up table in a second step. Therefore, an extra factor of 3 is added to the complexity of the MMSE-ASW algorithm. The required complexity of the MMSE equalization step is given in Table I. In case $D = 0$ is chosen by the MMSE-ASW, a simple ZF is applied with a complexity of 1 division operation i.e. 3 multiplications.

VII. SIMULATION RESULTS

In this section, we present simulation results for a DVB-T system [1], at a carrier frequency of 600MHz in a noise free environment. An 8k FFT is used in an 8MHz bandwidth with a guard interval of 2k samples. Out of the 8192 subcarriers, only 6048 carry data. 16QAM modulation is used on the OFDM subcarriers. A Viterbi convolutional channel decoder is used,

TABLE I
COMPLEXITY OF MMSE FILTERING APPLIED ON ONE SUBCARRIER

Step	Complexity (number of multiplications)
1-Multiplication $\mathbf{H}'(k)(\mathbf{H}'(k))^H$	$(2D+1)^3$
2-Inversion step $(\mathbf{H}'(k)(\mathbf{H}'(k))^H + \sigma^2 \mathbf{I})^{-1}$	$\frac{(2(2D+1)^3 + 3(2D+1)^2 - 5(2D+1))}{6}$
3-Multiplication of step 2 by $\mathbf{A}^H(k)$	$(2D+1)^2$
4- $\hat{S}(k) = \frac{1}{C(k)A(k)} C(k) \mathbf{R}_{(2D+1) \times 1}(k)$	$(2D+1) + (2D+1) + 3$

with a code rate of 2/3. We consider Doppler frequencies of 100Hz and 200Hz, which correspond to velocities of 180km/h and 360km/h, respectively. The simulated channel is a TU6 channel. A maximum value of $D_{max} = 2$ is set for the MMSE-ASW algorithm, which means the BER performance of the MMSE-ASW($D_{max} = 2$) can not be better than that of the conventional MMSE algorithm which uses $D = 2$ for all subcarrier signals. On the other hand, because MMSE-ASW is allowed to use $D = 2$ on some subcarriers, the BER performance can be better than that of a conventional MMSE receiver which uses $D = 1$ over all subcarriers. Pilot assisted channel estimation is conducted to obtain the main diagonal channel coefficients, using frequency only linear interpolation. In Figs. 5 and 6, the histograms of the chosen D by the ASW algorithm at different SIR_{min} are shown for Doppler frequencies of 100Hz and 200Hz, respectively. We notice that as the SIR_{min} increases, a higher D is chosen more frequently by the algorithm. In addition, we can see that for the same minimum threshold value SIR_{min} , as the Doppler frequency increases, the chosen D also increases, which is intuitively satisfying.

To be able to analyze both the BER performance and the

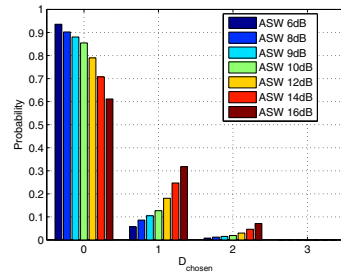


Fig. 5. Histograms of selected values of D based on (18) for different values of SIR_{min} at Doppler frequency=100Hz in a noise free environment

complexity of the proposed algorithm vs the classical MMSE approach, we consider Figs. 7 and 8. Every point in the plot carries information about the BER and complexity of MMSE-FWS (MMSE with fixed window size) or MMSE-ASW algorithms. The x-axis is the consumed complexity (number of multiplications) whereas the y-axis depicts the BER. At

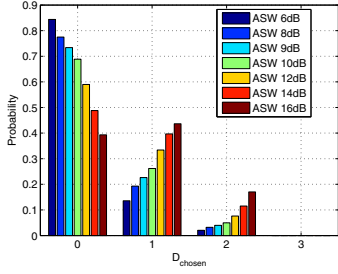


Fig. 6. Histograms of selected values of D based on (18) for different values of SIR_{min} at Doppler frequency=200Hz in a noise free environment

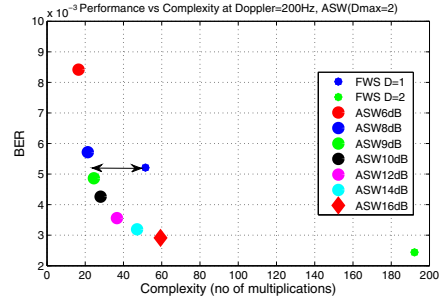


Fig. 8. BER vs complexity plot at a Doppler frequency of 200Hz and noise free environment

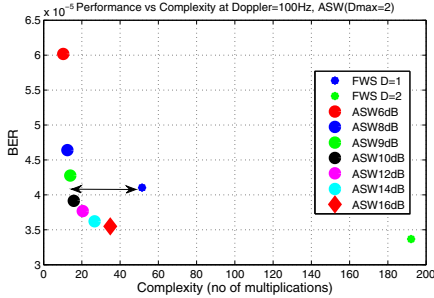


Fig. 7. BER vs complexity plot at a Doppler frequency of 100Hz and noise free environment

a Doppler frequency of 100Hz in Fig. 7, we observe the MMSE-ASW with $SIR_{min}=12,14$ and 16 dB has both better BER performance and less complexity compared to those of the conventional MMSE-FWS($D=1$). Using a threshold of 10 dB, only an average number of 16 multiplications are required as opposed to 51 multiplications needed with the conventional approach using fixed $D = 1$ for all subcarriers. Therefore, about 68% reduction in complexity can be achieved at a Doppler frequency of 100Hz using MMSE-ASW with $SIR_{min} = 10dB$. As the Doppler frequency increases in Fig. 8, MMSE-ASW on the one hand has the flexibility to choose higher values of D (up to $D_{max} = 2$). On the other hand, MMSE-FWS is forced to use $D = 1$ for all subcarriers, that is why lower threshold MMSE-ASW $SIR_{min} = 9dB$ can also exceed the overall performance of MMSE-FWS($D=1$) at high Doppler frequencies. Using MMSE-ASW with $SIR_{min} = 9dB$ requires only an average of 25 multiplications, therefore a 50% reduction in complexity can be achieved.

VIII. CONCLUSION

In this work, we have proposed an adaptive sliding window MMSE ICI canceller. We have shown that in a frequency selective channel, different subcarriers suffer from different interference distortion conditions. Therefore, allowing the canceller to choose a different window size for every subcarrier proved to be advantageous for frequency selective time-varying channels. We have analyzed BER performance and complexity trade-off in a DVB-T 8k OFDM system over a TU6 channel. Results have shown the advantages of

the proposed algorithm compared to a conventional MMSE equalizer with a constant window size. Using a threshold of 10dB, a 68% reduction of complexity was achieved compared to the conventional approach with a fixed value of $D = 1$ at almost the same BER. This was obtained at a Doppler frequency of 100 Hz, which corresponds to a user moving at a velocity of 180 km/h. In further work, the threshold, SIR_{min} , and the maximum allowed window size, D_{max} , can be also optimized depending on the channel model, e.g. for a given frequency selectivity. This idea can also be extended to other ICI cancellers, where different equalization settings should be considered for different subcarriers according to the interference conditions. Furthermore, the criteria for choosing $D(k)$ can also be optimized in noisy channels to include the signal to interference and noise ratio (SINR) instead of the SIR.

REFERENCES

- [1] ETSI, *ETSI EN 300 744 Digital Video Broadcasting (DVB); Framing structure, channel coding and modulation for digital terrestrial television*, Jan. 2009.
- [2] W. C. Jakes, *Microwave Mobile Communications*. Wiley, 1974.
- [3] J. van de Beek, M. Sandell, and P. Borjesson, "ML estimation of time and frequency offset in OFDM systems," *IEEE Transactions on Signal Processing*, vol. 45, no. 7, pp. 1800–1805, Jul. 1997.
- [4] S. Lu, R. Kalbasi, and N. Al-Dhahir, "OFDM Interference Mitigation Algorithms for Doubly-Selective Channels," in *IEEE 64th Vehicular Technology Conference VTC*, Sept. 2006, pp. 1–5.
- [5] K. Kim and H. Park, "A Low Complexity ICI Cancellation Method for High Mobility OFDM Systems," in *Vehicular Technology Conference, 2006. VTC 2006-Spring. IEEE 63rd*, vol. 5, May 2006, pp. 2528–2532.
- [6] K. Fang, L. Rugini, and G. Leus, "Low-Complexity Block Turbo Equalization for OFDM Systems in Time-Varying Channels," *IEEE Transactions on Signal Processing*, vol. 56, no. 11, pp. 5555–5566, Nov. 2008.
- [7] M. Russell and G. Stuber, "Interchannel interference analysis of OFDM in a mobile environment," in *IEEE 45th Vehicular Technology Conference*, vol. 2, Jul 1995, pp. 820–824.
- [8] S. M. Kay, *Fundamentals of statistical signal processing*, 1st ed. Prentice Hall, 1993.
- [9] "COST 207: Digital land mobile radio communications, Commission of the European Communities," Tech. Rep.
- [10] Y. Mostofi and D. Cox, "ICI mitigation for pilot-aided OFDM mobile systems," *IEEE Transactions on Wireless Communications*, vol. 4, no. 2, pp. 765–774, March 2005.